数理解析研究所講究録
第888巻 1994年 49-63

Dynamics of Vortical Structure in a Homogeneous Shear Flow

Shigeo Kida 木田重雄 RIMS, Kyoto University
Mitsuru Tanaka 田中満 Faculty of Science, Kyoto University

1. Introduction

The coherent structures, such as tubes and layers of concentrated vorticity, observed in fully developed turbulence have relatively long lifetimes. They are considered to play an essential role in turbulence dynamics. For example, the longitudinal vortex tubes oriented nearly along the mean flow direction play an important role in the production of turbulence energy in wall turbulence. Regeneration mechanism of longitudinal vortex tubes have been extensively investigated for this reason.[1-4] But their dynamics is not well understood yet and should be explored furthermore.

Here we consider a homogeneous shear flow, which is one of the simplest flows with non-zero mean flow profile. This would enable us to investigate vortical structures in detail. Several direct numerical simulations[5-9] revealed that vortical structures that are quite similar to those observed in a wall turbulence prevail also in homogeneous shear turbulence. Rogers and Moin[6] observed a hairpin-shaped vortical structure in a homogeneous shear flow with relatively weak strain. Lee *et al.*[7] made comparisons with the turbulent channel flows and found that if the mean shear rate is as strong as that in the buffer layer of a wall turbulence, the streak structures can appear even in the absence of a solid wall. There also exist longitudinal vortex tubes and vortex layers[8,9] which are observed in the wide range of shear strength and Reynolds number. Roughly speaking, there are two types of regeneration mechanisms of longitudinal vortex tubes in wall turbulence. One is phenomena which take place at a wall. The other is the inviscid one which may be attributed to the existence of a shear. In the research of homogeneous shear flows we can investigate the effects of shear on the generation of longitudinal vortex tubes separately from those of a wall.

In the present report we focus an attention to the vortical structures in a homogeneous shear turbulence and examine the generation, development and interactions of

them. In §2 we briefly describe our numerical simulations. We examine the statistical properties of vorticity vectors in §3 and interactions between longitudinal vortex tubes and vortex layers in §4.

2. Numerical Simulation

2.1 Basic Equation

We consider the motion of an incompressible viscous fluid in a linear mean shear

$$\boldsymbol{U} = (Sx_2, 0, 0), \tag{1}$$

which is along the x_1-direction and varies linearly with x_2 (Fig. 1). The mean vorticity $\boldsymbol{\Omega}$ is therefore uniform in space and is directed toward the negative x_3-axis, that is

$$\boldsymbol{\Omega} = (0, 0, -S). \tag{2}$$

Here, we call the x_1-, x_2- and x_3-axes the streamwise, vertical, and spanwise directions, respectively. Time-evolution of the fluctuating velocity $\boldsymbol{u}$ is described by the Navier-Stokes equation

$$\frac{\partial u_i}{\partial t} + Sx_2\frac{\partial u_i}{\partial x_1} + Su_2\delta_{i1} + u_k\frac{\partial u_i}{\partial x_k} = -\frac{\partial p}{\partial x_i} + \nu\nabla^2 u_i\,, \quad (i = 1,2,3) \tag{3}$$

supplemented by the continuity equation $\partial u_j/\partial x_j = 0$, where p is the pressure and ν is the kinematic viscosity of a fluid. The fluid density is assumed to be uniform and be unity. A summation is taken over 1 – 3 for repeated subscripts.

By taking the curl of (3), we obtain the equation for the fluctuating vorticity ($\boldsymbol{\omega} = \nabla \times \boldsymbol{u}$)

$$\frac{\partial \omega_i}{\partial t} = -\left(Sx_2\frac{\partial \omega_i}{\partial x_1} + u_k\frac{\partial \omega_i}{\partial x_k}\right) + \left(S\omega_2\delta_{i1} - S\frac{\partial u_i}{\partial x_3} + \omega_k\frac{\partial u_i}{\partial x_k}\right) + \nu\nabla^2\omega_i. \tag{4}$$

The first and the second terms in the first brackets on the rhs of (4) represent the advection of vorticity by the mean shear and the fluctuating velocity, respectively. Three terms in the second brackets describe a conversion of fluctuating vorticity by the mean shear, a conversion of the mean vorticity by the fluctuating field, and a conversion of fluctuating vorticity by the fluctuating field, respectively. Finally, the last term represents viscous diffusion.

2.2 Numerical Scheme and Initial Condition

Equation (3) is solved numerically in a coordinate system which is advected by the mean flow.[5] The computation is carried out on 128^3 grid points in a rectangular box of sides $4\pi \times 2\pi \times 2\pi$ by using the Fourier spectral/Runge-Kutta-Gill scheme. The initial velocity field is given with Fourier coefficients with random phase and with a prescribed energy spectrum of form $E(k) = c\,k^4 \exp[-2k^2/k_0^2]$, where c and k_0 are constants.

There are two non-dimensional parameters that characterize this problem. The shear rate parameter

$$S^* = \frac{u'^2/\epsilon}{1/S}$$

represents the ratio of the time-scale of the nonlinear interaction and that of the mean shear.[7] Here, u' is the rms of fluctuating velocity and ϵ is the mean energy dissipation rate. The Reynolds number

$$R_\lambda = \frac{u'^2/\epsilon}{1/\omega'}$$

represents the ratio of the time-scale of the nonlinear interaction and that of the viscous effects, where ω' is the rms of vorticity. We here report the numerical results for $S^*(0) = 16$ and $R_\lambda(0) = 16$.[8,9] The ratio of the rms of vorticity and the shear rate is 1 at the initial instant and therefore the mean strain and the nonlinear self-interaction may play comparable roles.

3. Vortical Structures and Vorticity Vectors

3.1 Vortical Structures in Homogeneous Shear Turbulence

Many complicated vortical structures develop and interact with each other in homogeneous shear turbulence. There are three typical vortical structures; the longitudinal vortex tubes nearly along to the streamwise direction, the lateral vortex tubes along the spanwise direction, and the vortex layers with spanwise vorticity. Here, the vortical structures are regarded as concentrated regions of vorticity.

The spatial structure of vorticity field is visualized with the iso-surface of vorticity magnitude. In Figs. 2 we plot iso-surfaces at $St = 0.4, 2, 8, 14$ in a cubic domain of sides $2\pi \times \frac{80}{128}$. The iso-surfaces at $St = 8$ and $St = 14$ are also seen from the x_2-direction in Figs.(e) and (f), respectively. The vorticity field is isotropic at the initial instant and regions of relatively high vorticity are seen as vorticity blobs (figures omitted). At earlier times ($St = 0.4$) high-vorticity blobs are being stretched in the direction inclined at 45^o to the downstream. Elongated high-vorticity regions are clearly seen at $St = 2$. These long thin high-vorticity regions are called longitudinal vortex tubes. At later times

the longitudinal vortex tubes incline more toward the streamwise direction. As shown in Figs. 2(c) and 2(e) high-vorticity regions at $St = 8$ exhibit layer-like structures. These vortex layers extend over several ten mesh-sizes in the streamwise direction and nearly ten mesh-sizes in the spanwise. Vorticity vectors in the layers are directed along the negative spanwise axis, that is, the direction of the mean vorticity. These vortical structures break down at further later stages (Fig. 2(e)). Lateral vortex tubes along the spanwise direction are also seen in Fig. 2(f).

Figure 3 shows the time-evolution of magnitude of each component of vorticity $\langle \omega_i^2 \rangle, i = (1,2,3)$, where $\langle\ \rangle$ denotes the spatial average. Enstrophy $\omega'^2 = \sum \langle \omega_i^2 \rangle$ increases almost exponentially in time, whereas the behavior of each element is quite complicated. In early stages ($0 \leq St \leq 2$) the streamwise component $\langle \omega_1^2 \rangle$ grows rapidly, which represents the generation and development of longitudinal vortex tubes. In this period the spanwise component $\langle \omega_3^2 \rangle$ is almost invariant in time since vorticity lines are not directly stretched in the spanwise direction by the mean shear. In the subsequent period ($2 \leq St \leq 5$) the streamwise component increases only slowly in time, suggesting that the development of longitudinal vortex tubes are balanced against viscous diffusion. The spanwise component, on the other hand, exhibits a rapid growth after $St = 2$, which corresponds to the development of the vortex layers. As will be discussed in §4, the spanwise component of vorticity is generated from the shear vorticity through a spanwise vortex stretching and therefore has the same sign as the mean vorticity. A rapid increase of the spanwise component is followed by a second rapid growth of the streamwise component. Finally, the streamwise component becomes larger than the spanwise. Longitudinal vortex tubes and vortex layers are observed as dominant vortical structures in the earlier stage ($0 \leq St \leq 6$) and in the middle stage ($6 \leq St \leq 12$), respectively, as indicated by the fact that the streamwise and spanwise components are the largest vorticity in the respective stages. At a further later stage longitudinal vortex tubes constitute the dominant structures again.

We have observed the following scenario of generation, development and breakdown of vortical structures (see ref. (9)).

(i) The linear mean shear flow stretches a randomly distributed initial vorticity field to generate longitudinal vortex tubes. These longitudinal vortex tubes are subsequently inclined more and more toward the streamwise direction increasing their strength. Vorticity vectors inside longitudinal vortex tubes are less inclined than the tubes themselves.

(ii) Strong longitudinal vortex tubes induce a strong swirling motion around them,

which stretches fluid elements in the spanwise direction most effectively to generate vortex layers with spanwise vorticity. Vortex layers are observed to be wrapped into longitudinal vortex tubes.

(iii) These vortex layers roll up into the lateral vortex tubes through the Kelvin-Helmholtz instability. These lateral vortex tubes are stretched and deformed into hairpin vortex tubes and longitudinal vortex tubes by the mean shear.

(iv) All of these typical structures break down into a disordered weak vorticity field through some instability mechanisms and complicated mutual-interactions.

Among these four processes, (ii) and (iii) are expected to play important roles in the formation of vortical structures, that is, longitudinal vortex tubes are intensified and regenerated by these processes. In the following we pay a special attention to the process (ii), that includes interactions between longitudinal vortex tubes and vortex layers.

3.2 Statistical Properties of Vorticity Vectors

In order to examine the distribution of direction of the vorticity vector quantitatively we introduce two orientation angles α and β, which are called the vertical and horizontal angles, respectively (Fig. 4). We have the following relations,

$$\begin{cases} \omega_1 = \omega \cos\alpha \sin\beta, \\ \omega_2 = \omega \sin\alpha, \\ \omega_3 = -\omega \cos\alpha \cos\beta, \end{cases} \tag{5}$$

where $\omega = |\boldsymbol{\omega}|$. Note that the origin $(\alpha, \beta) = (0^o, 0^o)$ corresponds to the negative x_3-axis, *i.e.* the direction of vorticity of the mean shear.

Suppose that $P(t, \boldsymbol{\omega})$ is a probability density function (pdf) of vorticity vectors $\boldsymbol{\omega}$ at time t. A pdf of the orientation angles of vorticity[6] weighted by ω^2 is give by

$$f(t, \alpha, \beta) \equiv c \int_0^\infty \omega^2 P(t, \boldsymbol{\omega}) \omega^2 \mathrm{d}\omega, \tag{6}$$

where c is a normalization factor.

The change in time of vorticity vectors may give helpful information for understanding of the dynamics of vortical structures. The time-evolution of the pdf is described by

$$\frac{\partial}{\partial t} P + \frac{\partial}{\partial \boldsymbol{\omega}} \left(\frac{\mathrm{D}\boldsymbol{\omega}}{\mathrm{D}t} P \right) = 0,$$

where $\mathrm{D}\boldsymbol{\omega}/\mathrm{D}t$ denotes the Lagrangian derivative of vorticity vectors which is calculated through the vorticity equation (4). The time-evolution of the pdf of orientation angles is represented in the spherical coordinate system (ω, α, β) by the equation

$$\frac{\partial}{\partial t} f = 2g_\omega - \frac{1}{\cos\alpha}\left\{\frac{\partial}{\partial \alpha}(g_\alpha \cos\alpha) + \frac{\partial}{\partial \beta} g_\beta\right\}, \tag{7}$$

where

$$\boldsymbol{g}(t, \alpha, \beta) \equiv c \int_0^\infty \omega \frac{\mathrm{D}\boldsymbol{\omega}}{\mathrm{D}t} P\omega^2 \mathrm{d}\omega \tag{8}$$

expresses the statistical change in time of direction of vorticity vectors pointing to the direction of $\boldsymbol{\omega}$. Notice that $2g_\omega$ represents the change in time of magnitude of vorticity vectors, that is, the production rate of enstrophy.

In order to get information about the change in time of direction of vorticity vectors we take time-derivatives of (5) to obtain the relationship between the time-derivative of vorticity vectors and orientation angles (α, β),

$$\frac{\mathrm{D}\alpha}{\mathrm{D}t} = \frac{1}{\omega}\left(-\frac{\mathrm{D}\omega_1}{\mathrm{D}t}\sin\alpha\sin\beta + \frac{\mathrm{D}\omega_2}{\mathrm{D}t}\cos\alpha + \frac{\mathrm{D}\omega_3}{\mathrm{D}t}\sin\alpha\cos\beta\right),$$
$$\frac{\mathrm{D}\beta}{\mathrm{D}t} = \frac{1}{\omega\cos\alpha}\left(\frac{\mathrm{D}\omega_1}{\mathrm{D}t}\cos\beta + \frac{\mathrm{D}\omega_3}{\mathrm{D}t}\sin\beta\right).$$

The movement of individual orientation angles may be expressed by the pdf of $\mathrm{D}\alpha/\mathrm{D}t$ and $\mathrm{D}\beta/\mathrm{D}t$ weighted by ω^2 as

$$\frac{\mathrm{d}\alpha}{\mathrm{d}t} \equiv \int_0^\infty \omega^2 \frac{\mathrm{D}\alpha}{\mathrm{D}t}\omega^2 \mathrm{d}\omega = \boldsymbol{n}_\alpha \cdot \boldsymbol{g}, \qquad \frac{\mathrm{d}\beta}{\mathrm{d}t} \equiv \int_0^\infty \omega^2 \frac{\mathrm{D}\beta}{\mathrm{D}t}\omega^2 \mathrm{d}\omega = \boldsymbol{n}_\beta \cdot \boldsymbol{g}, \tag{9}$$

where $\boldsymbol{n}_\alpha = (-\sin\alpha\sin\beta, \cos\alpha, \sin\alpha\cos\beta)$ and $\boldsymbol{n}_\beta = (\cos\beta, 0, \sin\beta)/\cos\alpha$ in the physical coordinate.

In Fig. 6 we show the weighted pdf of orientation angles of vorticity at $St = 0.4, 2, 8, 14$ (Eq.(6)). The pdf's for the fluctuating and the absolute vorticities are plotted in the left and the right sides, respectively. Here, the absolute vorticity is defined as $\boldsymbol{\omega}^T = \boldsymbol{\Omega} + \boldsymbol{\omega} = (\omega_1, \omega_2, \omega_3 - S)$. The distribution is symmetric with respect to the origin, which reflects the invariance of the flow configuration by a rotation of angle 180^o around the x_3-axis. The pdf is normalized so that the integral over the whole angle takes unity. Contour levels are $1, 2, 4, \cdots$.

First, we discuss the pdf for the fluctuating vorticity. At earlier times ($St = 0.4$), two peaks appear at $(\alpha_{\mathrm{peak}}, \beta_{\mathrm{peak}}) = \pm(45^o, 90^o)$ which are the directions of the

maximal expansion of the mean shear $(Sx_2, 0, 0)$.[6] As time goes on, the peaks become sharper, representing longitudinal vortices are being generated. They move toward $(\alpha, \beta) = (0^o, \pm 180^o)$. The decrease of $|\alpha|$ represents that the fluctuating vorticity tends to incline toward the streamwise direction, while the increase of $|\beta|$ means that they are turned to the opposite to the vorticity of the mean shear. A mechanism of the change in direction of vorticity vector were investigated in ref. (9). The positions of the peaks eventually stay around $(\alpha_{\rm peak}, \beta_{\rm peak}) = \pm(20^o, 130^o)$. These statistically equilibrium angles should be maintained by some complicated dynamics of vortical structures.

In a later period there appears two peaks at $(\alpha^{\rm T}_{\rm peak}, \beta^{\rm T}_{\rm peak}) = \pm(20^o, 90^o)$ in the pdf for the absolute vorticity, which also corresponds to the longitudinal vortex tubes. It is interesting that the horizontal peak angle $\beta^{\rm T}_{\rm peak}$ is $\pm 90^o$, *i.e.* the absolute vorticity in the longitudinal vortex tubes are aligned perpendicularly to the mean vorticity. No clear-cut explanation exists, however.

In the pdf for fluctuating vorticity there appears another peak around the origin at $St = 8$, which disappears at $St = 14$. This peak corresponds to vortex layers generated around this period (see §4). Vorticity vectors corresponding to this peak are pointed to the direction of the mean shear vorticity. This peak is thin in horizontal angle β and wide in vertical angle α, which reflects wavy vortex layers in which the vorticity is perpendicular to longitudinal vortex tubes.

Next, we examine the change in time of vorticity vectors. We consider the pdf for absolute vorticity. In Fig. 6(a) we plot the production rate of enstrophy $2g_\omega$ at $St = 8$. Positive regions are shaded. The pdf is normalized so that the total volume takes unity as in the pdf of orientation angles. Note that $\mathrm{D}\omega^2/\mathrm{D}t > 0$ (see Fig. 3). Contour levels are $1, 2, 4, \cdots, -1, -2, \cdots$. Vorticity is strengthened in the positive region around the origin and is weakened in negative regions around the peaks corresponding to the longitudinal vortex tubes $(\alpha, \beta) = (\pm 20^o, \pm 90^o)$. The pdf takes very large values at the origin, which means that vorticity vectors oriented in the direction of the mean vorticity are most effectively stretched. On the other hand, the magnitude of vorticity vectors in longitudinal vortex tubes tends to decrease in time. In fact, the stretching terms in the second brackets in the rhs of (4) amplify in average all the vorticity vectors. In the negative regions, however, the effect of viscosity dominates that of the stretching.

Now, we consider the change in time of direction of vorticity vectors. In Fig. 6(b) we plot the pdf of time-derivative field $(\mathrm{d}\alpha/\mathrm{d}t, \mathrm{d}\beta/\mathrm{d}t)$ of the orientation angles at $St = 8$. The length of arrows represents the square root of the magnitude of time-derivative

vectors. Contour lines of the pdf of the orientation angles are shown for reference (see Fig. 5). The flow in the vector field has a peculiar feature. It migrates from the origin to the right and left along a line $\beta^{\mathrm{T}} = 0$ up to $|\alpha^{\mathrm{T}}| = 40^o \sim 90^o$. Then the flow changes its direction toward larger $|\beta^{\mathrm{T}}|$ until $|\beta^{\mathrm{T}}| = 90^o \sim 120^o$. Remember that the pdf of the orientation angles has peaks at $(\alpha^{\mathrm{T}}_{\mathrm{peak}}, \beta^{\mathrm{T}}_{\mathrm{peak}}) = \pm(20^o, 90^o)$ which roughly represents the mean orientation of longitudinal vortex tubes. The flow turns around these peaks and approaches $(\alpha^{\mathrm{T}}_{\mathrm{peak}}, \beta^{\mathrm{T}}_{\mathrm{peak}}) = \pm(0^o, 90^o)$. This flow pattern is commonly observed at other times ($St > 2$).

Figure 6(c) illustrates the change in time of vorticity vectors in the physical space. Here, solid and blank arrows denote the directions of vorticity vectors and their time-evolution. First, the vorticity vectors oriented to the direction of the mean vorticity are inclined toward the x_2-direction. After they are inclined at $40^o \sim 90^o$ to the negative spanwise direction, they start turning toward the positive x_3-direction, *i.e.* the opposite to the mean vorticity. While the spanwise component of absolute vorticity ω_3^T approaches zero, it begins to lean toward the x_1-direction. Taking the results in Figs. 6(a) and 6(b) into account, we understand that the vorticity generated around the direction of the mean vorticity is transferred to the streamwise direction and is dissipated there. Equation (7) gives the change in time of the pdf of the orientation angles. The first and the second terms in the rhs of (7) represent the contribution from vortex stretching and tilting, respectively. The first term dominates the second around the origin, whereas they are comparable around the peaks corresponding to the longitudinal vortex tubes.

4. Interactions between Longitudinal Vortex Tubes and Vortex Layers

4.1 Development of Vortex Layers due to Pairs of Longitudinal Vortex Tubes

We consider here a mechanism of generation of vortex layers which are observed in the iso-vorticity surfaces (Fig. 2(c, e)). Figure 7 illustrates a generation mechanism. Longitudinal vortex tubes induce straining flows perpendicular to themselves. These straining flows distort the vorticity field in a random way, which in average stretches fluid elements. The spanwise component of absolute vorticity dominates the other components, since the mean vorticity is along the negative spanwise axis. Therefore, the stretching in the spanwise direction may most effectively contribute to magnify vorticity (Fig. 6(a)). Indeed a single vortex or a pair of vortices can generate shear flows, but

an extremely strong spanwise expansion can be generated by combined effects of two pairs of vortex tubes arranged as shown schematically in Fig. 7. If they happen to be arranged in this way, a strong vortex layer with spanwise component of vorticity is generated between them. In Figs. 8 we plot the streamwise vorticity ω_1 on the (x_3, x_2) plane. It is positive (in clockwise rotation) in white regions, while it is negative (in counterclockwise rotation) in dark regions. The vorticity and velocity perpendicular to the plane are represented by lines in Figs. 8(a) and 8(b), respectively. A thin horizontal region of concentrated vorticity in the center of Fig. 8(a) represents the cross-section of a large vortex layer seen in Fig. 2(e). It is clearly seen that the vortex layer is being intensified due to the straining flows (spanwise expansion) induced by four (two negative and two positive) longitudinal vortex tubes.

4.2 Wrapping of Vortex Layer into Longitudinal Vortex Tube

The movement of vorticity vector as shown in Fig. 6(c) may represents a wrapping process of vortex layers into longitudinal vortex tubes. In Figs. 9 we sketch a longitudinal vortex tube and a vortex layer. Figure 9(b) represents a cross-section of the structure. The longitudinal tube and the layer are oriented nearly to the streamwise direction (see Figs. 2). The mean flow comes out of the page and the mean vorticity points to the right. As shown in Fig. 5 the absolute vorticity vectors point to the direction of the mean vorticity in the vortex layer and are nearly aligned with the structure in the longitudinal vortex tube. The layer is deformed by the flow induced by the longitudinal vortex tube as shown in Fig. 9(b). At the same time vorticity vectors in the layer are turned toward the x_2-direction and then to the positive x_3-direction. The mean flow increases vertically, which inclines the vorticity vectors toward the x_1-direction (see also a discussion in §5). This is typically an inviscid phenomenon (remember that vorticity lines are material in an inviscid fluid). Such behavior of vorticity vectors is consistent with the change illustrated in Fig. 6(c). In short, vorticity vectors are tilted toward the streamwise direction rotating around the longitudinal vortex tubes.

It is seen in Figs. 8 that a vortex layer in the center is being wrapped into a longitudinal vortex tube, one of the four vortex tubes that contribute to the development of the vortex layer. A three dimensional view of Figs. 8 is drawn in Fig. 10. Grey regions ($\omega_3^T \leq -5S$) and black regions ($\omega_1 \leq -3.2S$) correspond to the vortex layer and the strongest longitudinal vortex tube in Fig. 8, respectively. Black lines represent the absolute vorticity lines starting at points in the vortex layer which are denoted by spheres. The longitudinal vortex tube rotates in counterclockwise direction. Remember

that the flow configuration is invariant under a 180°-rotation around x_3-axis. It is clearly seen that inside the vortex layer vorticity lines are tilted toward the $-x_2$-, x_3-, and then to the $-x_1$-directions. A similar behavior of vorticity lines is observed in a turbulent boundary layer.[1]

5. Summary and Discussions

We have examined interactions between longitudinal vortex tubes and vortex layers. Longitudinal vortex tubes induce straining flows around them, which stretches fluid elements in the spanwise direction most effectively to generate vortex layers with spanwise vorticity. An extremely strong spanwise expansion of fluid elements can be induced effectively by combined effects of two pairs of vortex tubes arranged as shown schematically in Fig. 7. Most of spanwise vorticity is created by this process. Since longitudinal vortex tubes induce swirling motions perpendicular to themselves, vorticity lines thus stretched are tilted toward the x_2-direction. Generation of vertical vorticity ω_2 is mainly due to the rotation of vorticity lines (in vortex layers) around longitudinal vortex tubes. Since the mean shear converts vorticity from the vertical to the streamwise components (see the first term in the second brackets in the rhs of (4)), the vertical vorticity may be regarded as a source of the streamwise vorticity.

The generation mechanism of the streamwise vorticity, however, seems to be quite complicated. Suppose that longitudinal vortex tubes are aligned along the direction inclined at $\alpha \approx 20^o$ to the streamwise axis. We introduce a new coordinate system (x_s, x_n, x_3) along the structure. The time-evolution of the structural component of vorticity ω_s is governed by

$$\frac{\mathrm{D}\omega_s}{\mathrm{D}t} = S\left(\omega_s \sin\alpha\cos\alpha - \omega_n \sin^2\alpha - \frac{\partial u_3}{\partial x_s}\cos^2\alpha\right) + \omega_s\frac{\partial u_s}{\partial x_s} - \frac{\partial u_s}{\partial x_n}\frac{\partial u_3}{\partial x_s} + \frac{\partial u_s}{\partial x_3}\frac{\partial u_n}{\partial x_s} + \nu\nabla^2\omega_s. \tag{10}$$

If the fluctuating field is uniform in the structural direction, eq.(10) is reduced to (neglecting the viscous term)

$$\frac{\mathrm{D}\omega_s}{\mathrm{D}t} = S\omega_1 \sin\alpha. \tag{11}$$

This tells us that the structural component of vorticity can be created only if vortical structures (vortex layers) contain the streamwise component of vorticity. Therefore, a conversion of vorticity from vertical to streamwise components should be caused by non-uniformity in the x_s-direction rather than the vertical inclination of the structure to the streamwise direction. The third term in the rhs of (10) seems to play an important

role, especially in the regions of large ω_2 which corresponds wavy vortex layers. Vortex layers deformed as shown in Fig. 9(b) may be stretched in the streamwise direction by this term, when they are modulated in the streamwise ($\approx$ structural) direction or are kinked in the spanwise direction.

It is desirable to examine how the growth of ω_1 leads to the generation of longitudinal vortex tubes. There are several regeneration processes of longitudinal tubes observed so far: a wrapping of vortex layers into longitudinal vortex tubes,[1] a roll-up of vortex layers into lateral vortex tubes and their subsequent deformation to hairpin vortices,[4,9] a roll-up of vortex layers in which streamwise component of vorticity is magnified while they are inclined toward streamwise direction.[10] It may be of primary importance to verify which one is dominant.

References

[1] J. Jiménez and P. Moin, "The minimal flow unit in near-wall turbulence," J. Fluid Mech. **225** (1991) 213.

[2] J.W. Brooke and T.J. Hanratty, "Origin of turbulent-producing eddies in a channel flow," Phys. Fluids A **5** (1993) 1011.

[3] P.S. Bernard, J.M. Thomas and R.A. Handler, "Vortex dynamics and the production of Reynolds stress," J. Fluid Mech. **253** (1993) 385.

[4] N.D. Sandham and L. Kleiser, "The late stages of transition to turbulence in channel flow," J. Fluid Mech. **245** (1992) 319.

[5] R.S. Rogallo, "Numerical experiments in homogeneous turbulence", NASA Tech. Memo. 81315 (1981).

[6] M.M. Rogers and P. Moin, "The structure of the vorticity field in homogeneous turbulence flows", J. Fluid Mech. **176** (1987) 33.

[7] M.J. Lee, J. Kim, and P. Moin, "Structure of turbulence at high shear rate", J. Fluid Mech. **216** (1990) 561.

[8] S. Kida and M. Tanaka, "Reynolds stress and vortical structure in a uniformly sheared turbulence", J. Phys. Soc. Jpn. **61** (1992) 4400.

[9] S. Kida and M. Tanaka, "Dynamics of vortical structures in a homogeneous shear flow", J. Fluid Mech. (1994) (in print).

[10] J. Jiménez and P. Orlandi, "The rollup of a vortex layer near a wall", J. Fluid Mech. **248** (1993) 297.

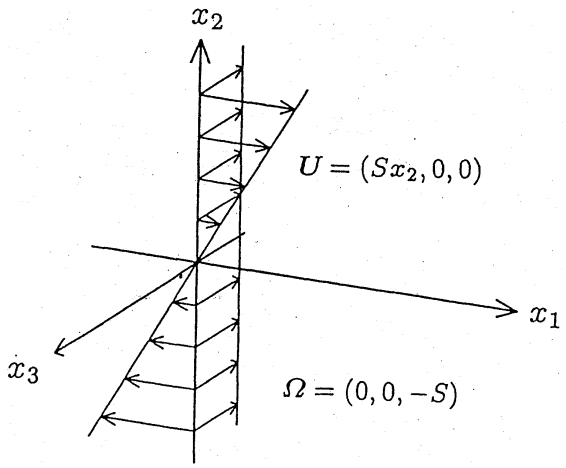

Fig. 1. Configuration of homogeneous shear flow.

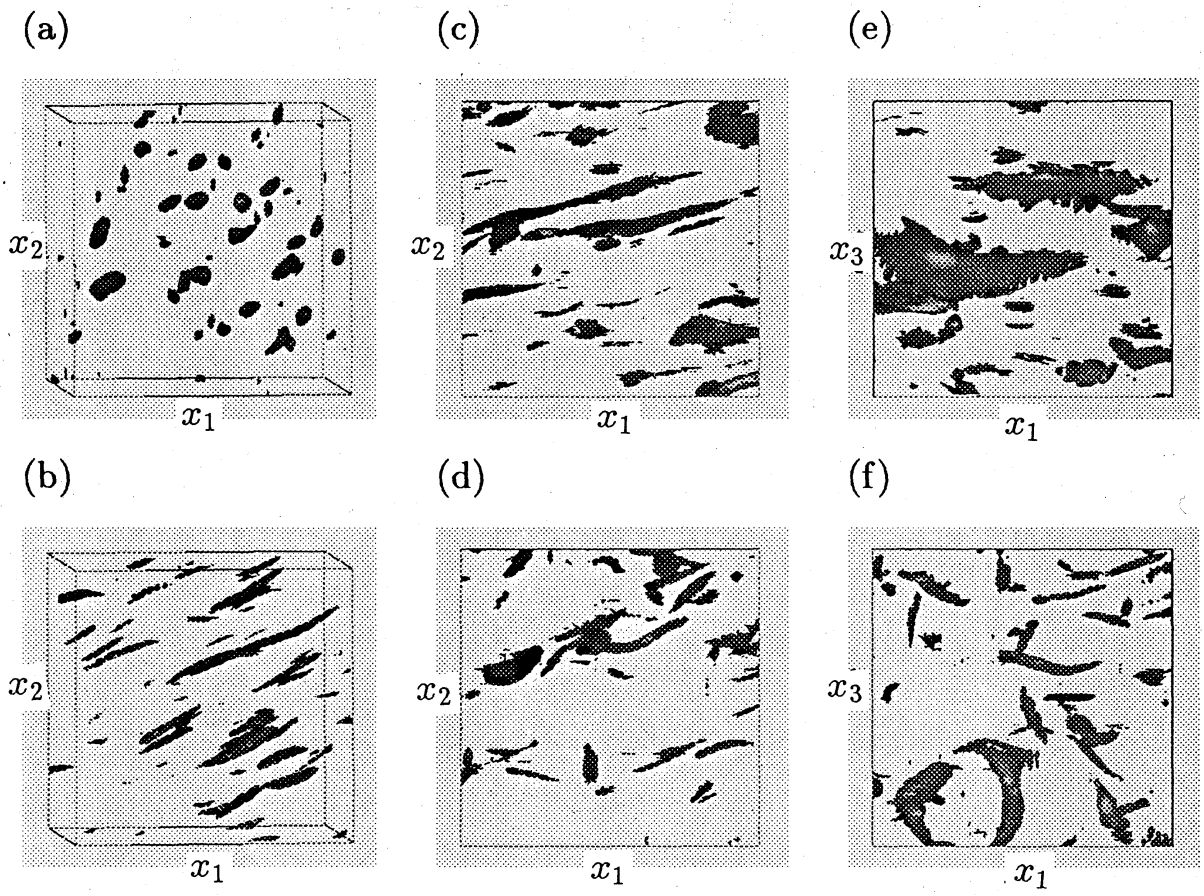

Fig. 2. Iso-surfaces of vorticity magnitude. (a) $St = 0.4$, $0 \leq x_1/\Delta x_1 \leq 40, 0 \leq x_2/\Delta x_2 \leq 80, 0 \leq x_3/\Delta x_3 \leq 80$, $|\boldsymbol{\omega}| = 2.2S = 2.2\omega'$, (b) $St = 2$, $20 \leq x_1/\Delta x_1 \leq 60, 0 \leq x_2/\Delta x_2 \leq 80, 0 \leq x_3/\Delta x_3 \leq 80$, $|\boldsymbol{\omega}| = 3.2S = 2.5\omega'$, (c) $St = 8$, $65 \leq x_1/\Delta x_1 \leq 105, 40 \leq x_2/\Delta x_2 \leq 120, 30 \leq x_3/\Delta x_3 \leq 110$, $|\boldsymbol{\omega}| = 4.5S = 2.4\omega'$, (d) $St = 14$, $45 \leq x_1/\Delta x_1 \leq 85, 47 \leq x_2/\Delta x_2 \leq 127, 47 \leq x_3/\Delta x_3 \leq 127$, $|\boldsymbol{\omega}| = 8.9S = 3.0\omega'$. Iso-surfaces at (e) $St = 8$ and at (f) $St = 14$ are viewed from the x_2-direction.

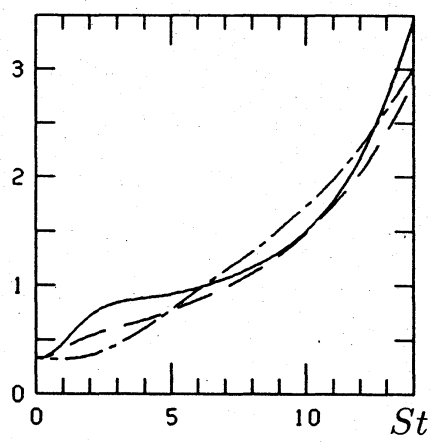

Fig. 3. Time-evolution of magnitudes of vorticity components $\langle\omega_i^2\rangle$. —, $\langle\omega_1^2\rangle$; - - -, $\langle\omega_2^2\rangle$; — · — · —, $\langle\omega_3^2\rangle$.

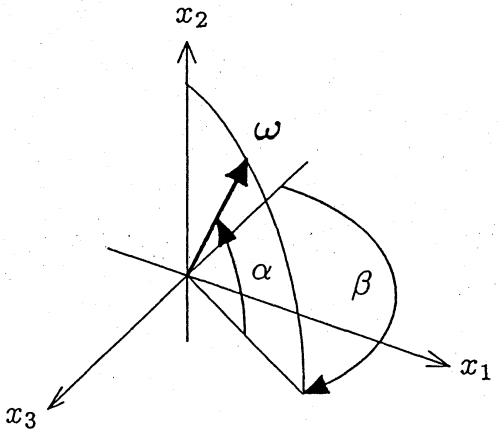

Fig. 4. Two orientation angles α and β.

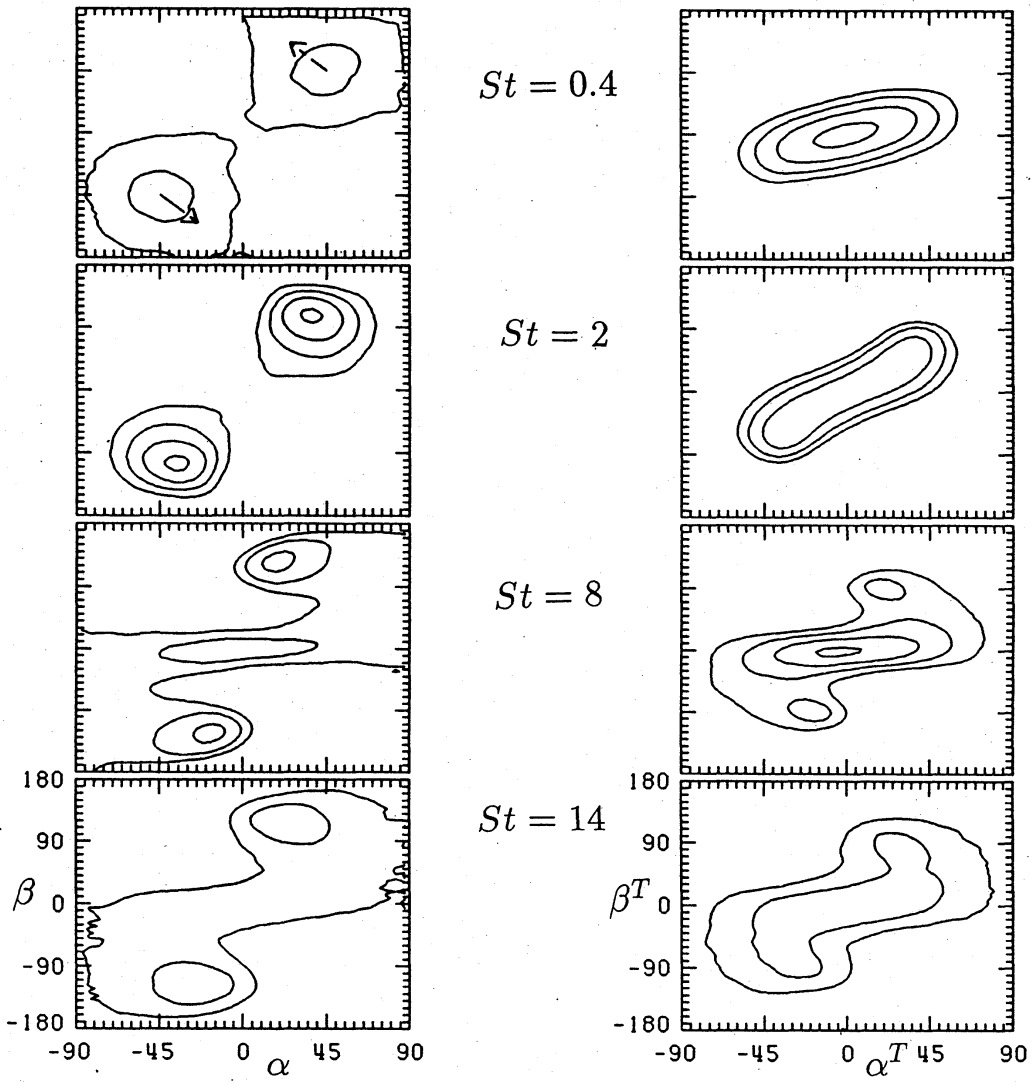

Fig. 5. Pdf of orientation angles of fluctuating (left) and absolute (right) vorticities.

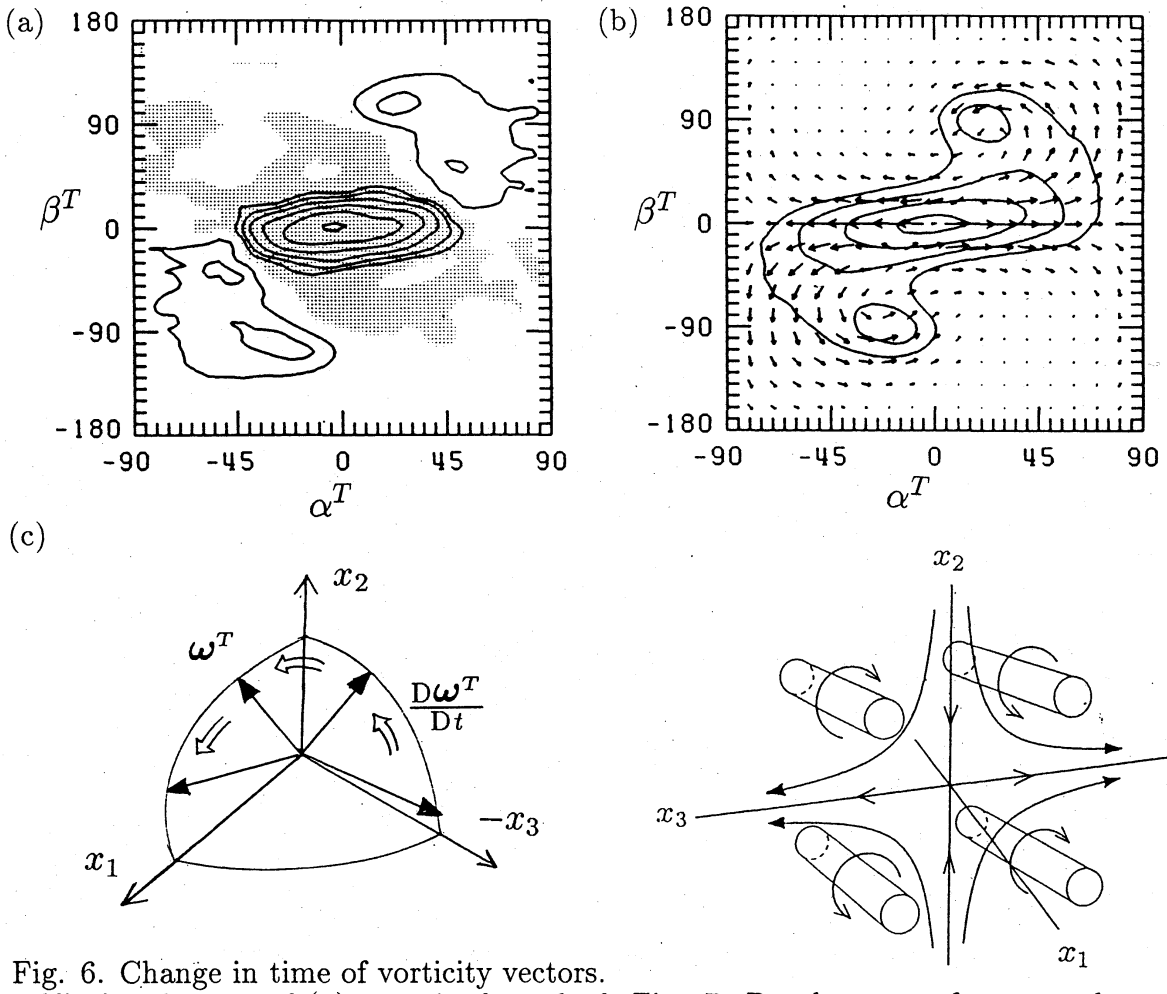

Fig. 6. Change in time of vorticity vectors. Pdf's for changes of (a) magnitude and of (b) direction. (c) Change in the physical space.

Fig. 7. Development of a vortex layer due to the straining flow induced by longitudinal vortex tubes.

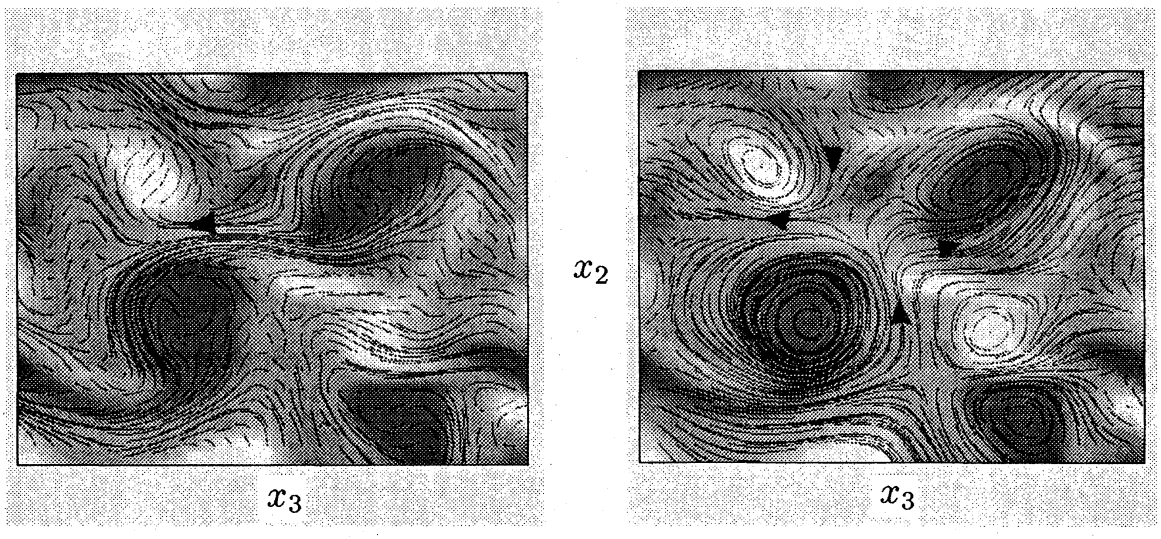

Fig. 8. Distribution of ω_1 in the (x_3, x_2) plane with (a) the vorticity and (b) the velocity field perpendicular to the plane.

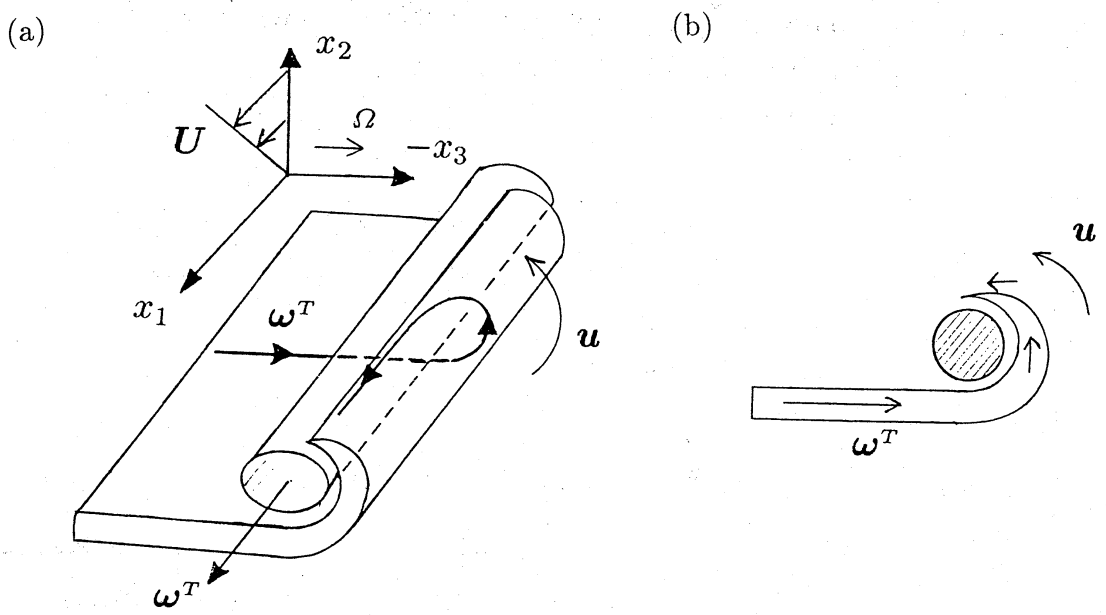

Fig. 9. Sketch of wrapping of a vortex layer into a longitudinal vortex tube.

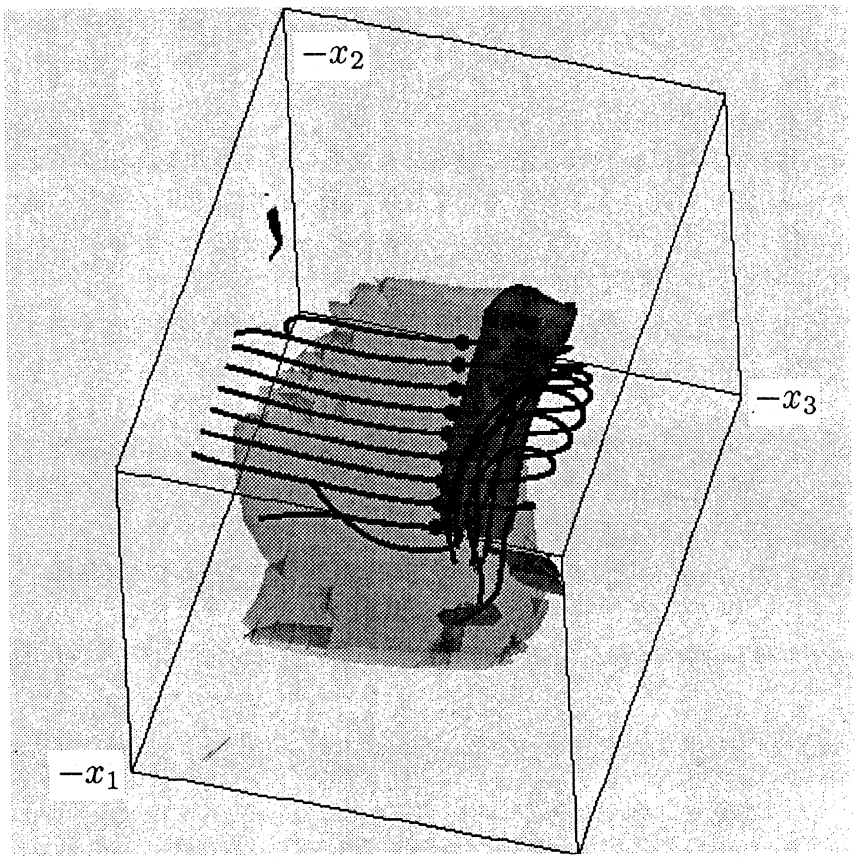

Fig. 10. Three dimensional view of wrapping of vortex lines. $St = 8$. Black and grey represent regions $\omega_1 \leq -3.2S$ and $\omega_3^T \leq -5S$, respectively. $8 \leq x_1/\triangle x_1 \leq 25, 0 \leq x_2/\triangle x_2 \leq 25, 5 \leq x_3/\triangle x_3 \leq 30$.